gram has been carried on with the cooperation of District Airway Engineers E.F. Cooke, John H. Curzon, Homer P. Keith, W.C. MacDonald, George W. Smith, and A.L.H. Somerville.

The base course and subgrade samples from the different airports were tested at the University of Alberta under Dean R.M. Hardy, at McGill University under G.A. Leonards, and at the University of Toronto under Professor R.F. Legget assisted by R.L. Davies.

The excellent cooperation from everyone associated with the investigation has been warmly appreciated, and special mention should be made of the able assistance provided by C.L. Perkins, J.P. Walsh, D.S. Johnson, P.J.Prokopy, R. Applebaum, and B.H. Newington, in working up and correlating the data.

-o-o-o-o-o-o-

SUB-SECTION VIII c

METHODS OF RIGID PAVEMENT DESIGN

VIII c 3 CALCULATION OF STRESSES IN ROAD AND RUNWAY CONSTRUCTIONS

M. DE KRUYF

C. v.d. POEL

R. TIMMAN

Laboratory N.V. De Bataafsche Petroleum Maatschappij

SUMMARY.

A method is given to calculate the stresses occurring in a road- or runway construction under static load. The method was specially developed for calculating the "sandwich" runway construction on Schiphol airfield, but allows of much wider application. A more complete solution for the problem of an elastic slab on subsoil is offered than was given by Hertz and Westergaard. This solution also enables the maximum stresses for the case of dual-wheel loading to be calculated. The results are laid down in figures, which can be used without further mathematical knowledge of the problem.

1. OBJECT

As mentioned in paper no. VIII d 4, the "sandwich" runway construction on Schiphol airport consists of a 30 cm cement concrete slab in direct contact with the subsoil. This slab is superimposed by a sand layer (35 cm) and a stone foundation (25 cm Telford layer) which is covered with a 5 cm asphaltic concrete layer.

The object of the study is to calculate the maximum tensile stress occurring in the concrete slab and its deflections when this construction is loaded on top.

2. PRESSURE DISTRIBUTION ON TOP OF CEMENT-CONCRETE SLAB.

First, the pressure distribution in the upper side of the cement-concrete slab Allowance must be made for the fact that the rigidity of the upper layers is very low in comparison with that of the concrete slab.

Cummings 3) calculated the stresses in an elastic layer (thickness z) with a rigid underlying boundary. The normal pressures caused on this rigid boundary can be computed from a rather complicated formula.

According to Terzaghi 4), however, practically the same result is obtained if Boussinesq's formula is applied, provided $\frac{2}{3}$ z is substituted for z. This holds good both for the point under the centre of the loaded area and for points outside it (i.c. page 421).

The latter method has been adopted here. For the determination of the pressures use was made of Newmark's 5) "grid" method. With this graphical method the pressures outside the centre loading of could be determined even more easily and accurately than by calculation with formulae containing expansions of a series.For details about this method we refer to the literature. The result is given in fig. 1 showing curves for single and for dual wheels. Loads and pressures are taken in accordance with P.I.C.A.O. recommendations of 1945 and 1946 for class A airfields.

3. STRESSES AND DEFLECTIONS IN CEMENT CONCRETE SLABS

We now come to the main problem of calculating the stresses in a elastic slab ona subsoil when the pressure distribution in the upper side is known. The simplest mathematical formulation of this problem is found if the counterpressure of the soil is put directly proportionality constant, the so-called modulus of subgrade reaction.

A partial solution was already given by Hertz in 1384 1) afterwards put in a more modern form by Westergaard 2). Both give formulae holding good for the case of a homogeneous pressure distribution over a circular area.They obtain this result by intergration of the solution for loading in a single point and consequently it was only possible to calculate the stress under the centre of the loaded area.

For single-wheel loading this knowledge

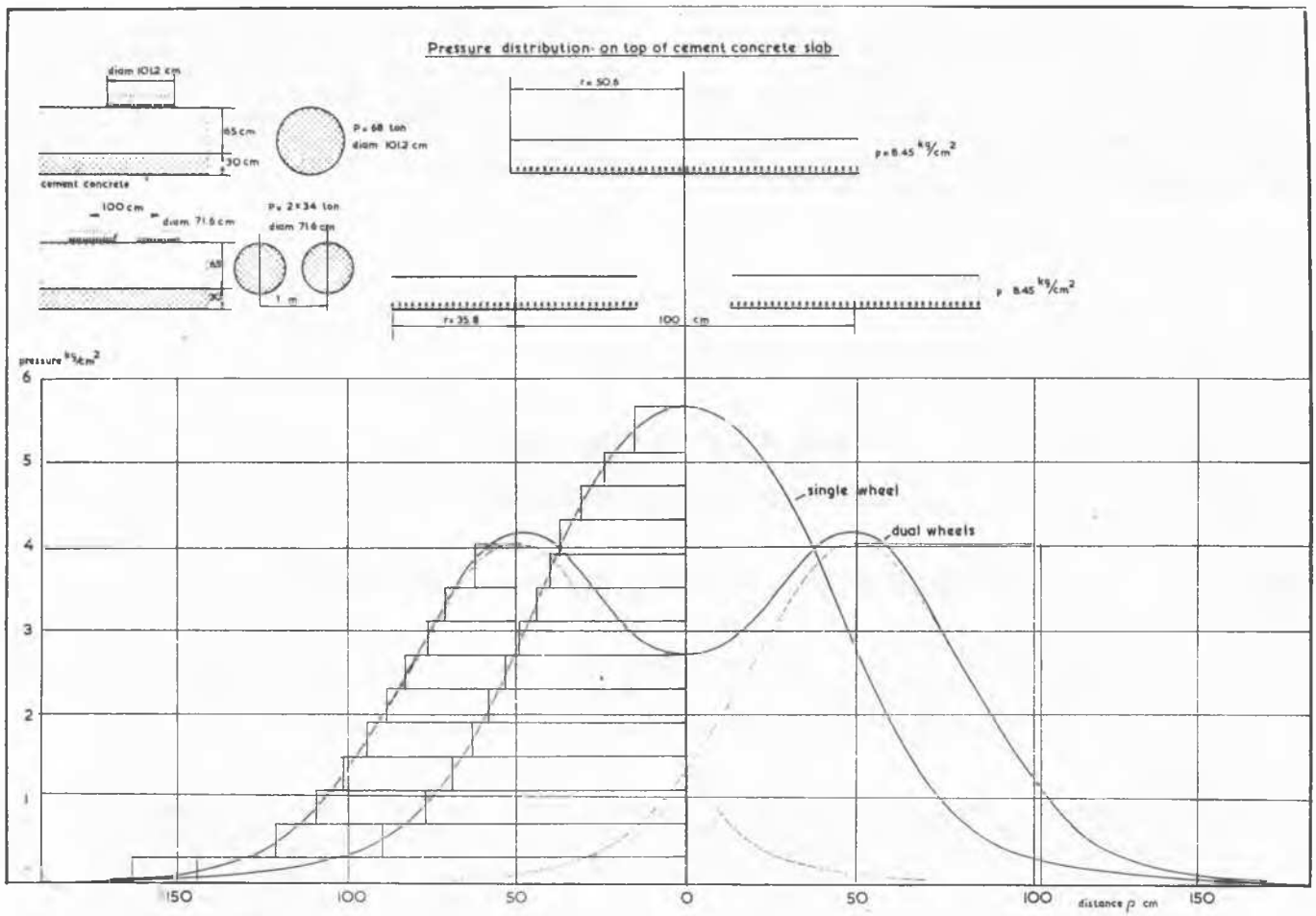

FIG. 1

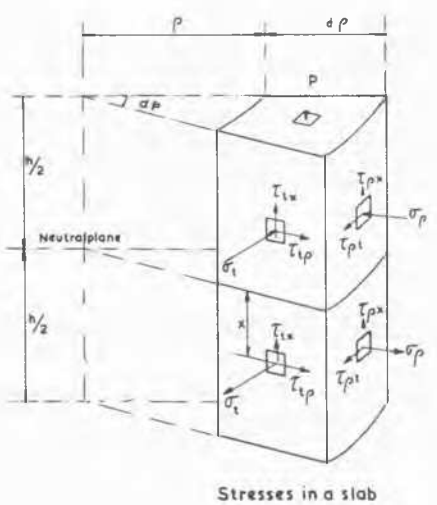

FIG. 2

will suffice, because in that case the stress under the load centre is at the same time the maximum stress. With dual-wheel loading this is it necessary to know the stress in the slab at any distance (ρ) from the centre.

In the last section of this paper we give the complete solution of the problem including explicit formulae for calculating stresses and deflections. From these formulae the solution of Hertz - Westergaard emerges as a special case.

The results of the calculations are digested in simple graphs which are suited for practical use, and which we will discuss here without going into the mathematical side.

With the aid of an element from the slab we will now first consider what stresses may occur in it (see fig. 2). The element, which has been chosen according to cylinder coordinates, has infinitesimal dimensions $d\rho$ and $\rho\, d\varphi$, but a finite height h equal to the thickness of the slab.

The various stress components have been drawn in the planes visible in the figure. It will be seen that there are two normal stress components, one in tangential direction (σ_t) and one in radial direction (σ_ρ). Both these stresses increase linearly with the distance x from the neutral plane and are maximum at the upper and lower surfaces of the slab. Since we wish to know the maximum tensile stress, we will from now on use the symbols σ_t and σ_ρ for the stress at the planes $x = \pm \frac{1}{2} h$.

In the case of radial symmetry the shearing stresses $\tau_{\rho t}$ and $\tau_{t\rho}$ are zero throughout the planes and need not be considered.

The shearing stresses τ_{tx} and $\tau_{\rho x}$ reach a maximum in the neutral plane and are zero for $x = \frac{1}{2}h$, as the boundary planes of the slab are supposed to be free from shearing stresses.

Consequently for $x = \pm \frac{1}{2}h$ there are only compression or tensile stresses on the planes in fig. 2 and σ_t, σ_ρ and p are principal stresses.

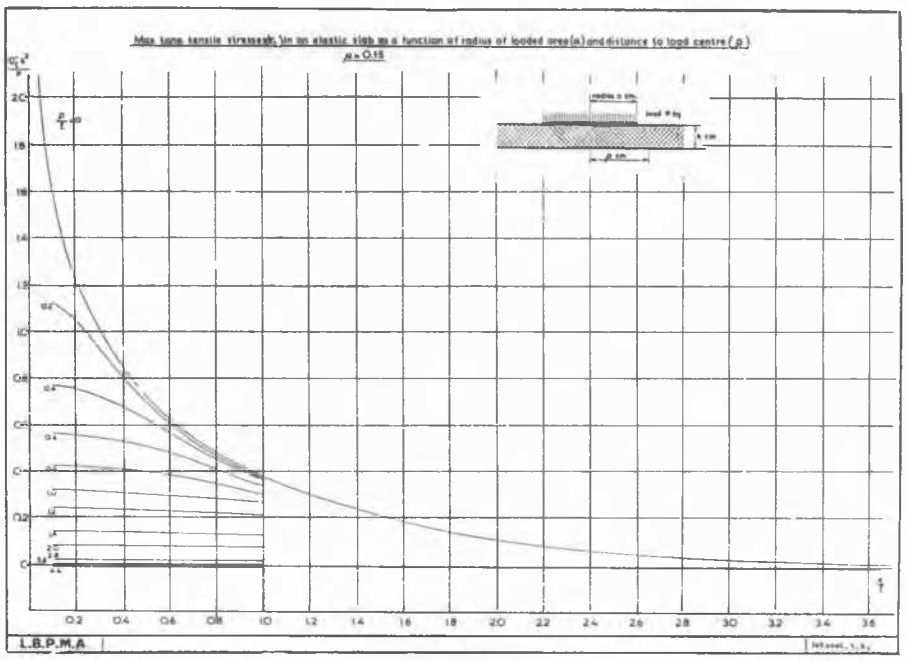

FIG. 3

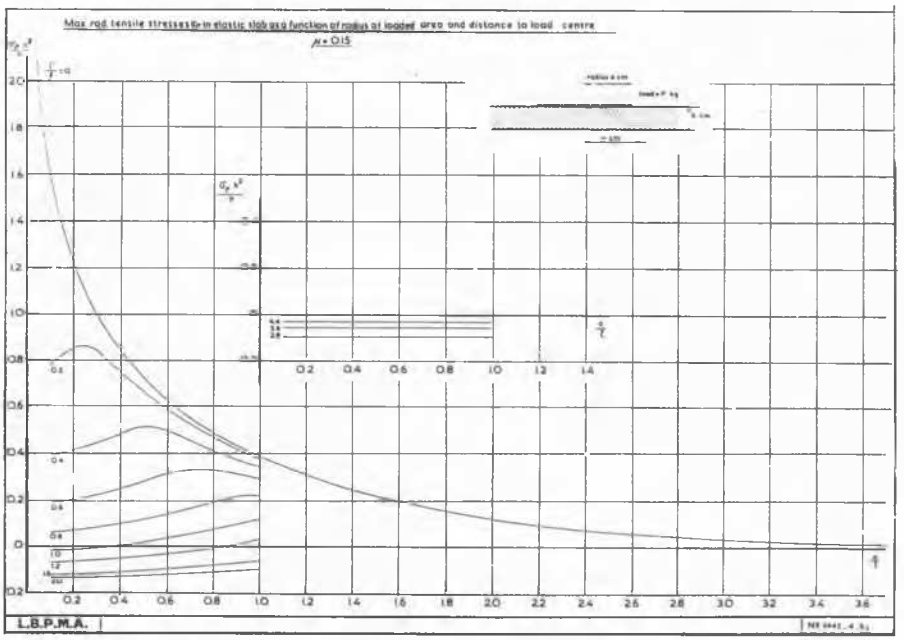

FIG. 4

As will be seen below, this conclusion is of great importance.

The values of σ_t and σ_ρ have been calculated for the case that the load P on top of the slab is uniformly distributed over circular area with radius a.

The results of these calculations are digested in figs 3, 4 and 5, from which the dimensionless magnitudes for the stresses $\frac{\sigma_t h^2}{P}$ and $\frac{\sigma_\rho h^2}{P}$ can be read off as functions of the dimensionless magnitudes for the radius of the loaded area $\frac{a}{\ell}$ and the distance from the centre of this area $\frac{a}{\ell}$.

ℓ is determined by the formula:

$$\ell = \sqrt[4]{\frac{m^2 E}{m^2 - 1} \cdot \frac{h^3}{12} \cdot \frac{1}{k}} \qquad (3,1)$$

where E is Young's modulus and $m = \frac{1}{\mu}$ Poisson's constant for the concrete and k is the modulus of subgrade reaction for the subsoil.

Figs. 3 and 4 do not differ essentially from 5; in the former $\frac{\rho}{\ell}$ is a parameter, in the latter this is $\frac{a}{\ell}$. Graphs 3 and 4 are best suitable for the low and graph 5 for the high values of $\frac{\rho}{\ell}$.

Under the load centre ($\frac{\rho}{\ell} = 0$) σ_ρ and σ_t are equal, and the solution is identical with that given by Westergaard 2). (See also the last section). The new point appears with the curves for other values of $\frac{\rho}{\ell}$.

Finally, the deflections of the neutral plane can also be computed. For formulae and derivation we would again refer to the last section.

The deflection under the centre of the load for the case of a point load amounts to:

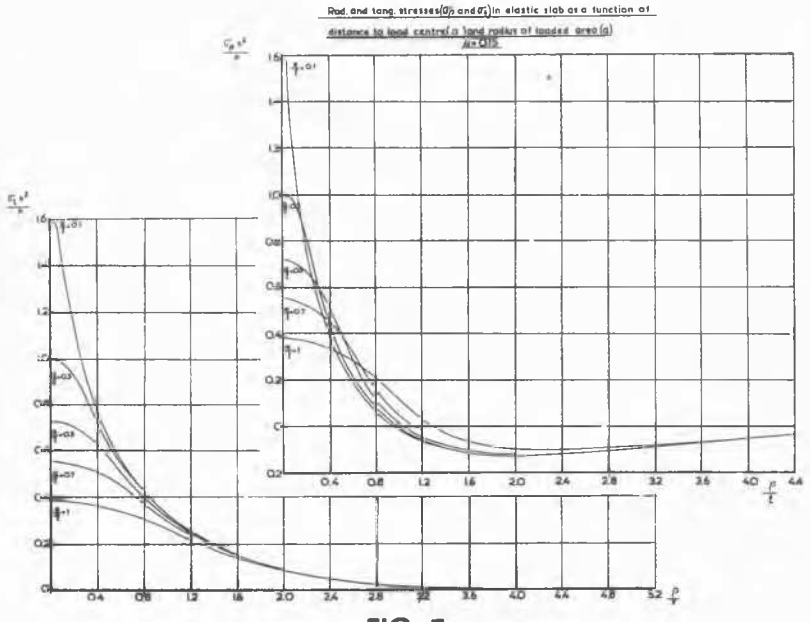

FIG. 5

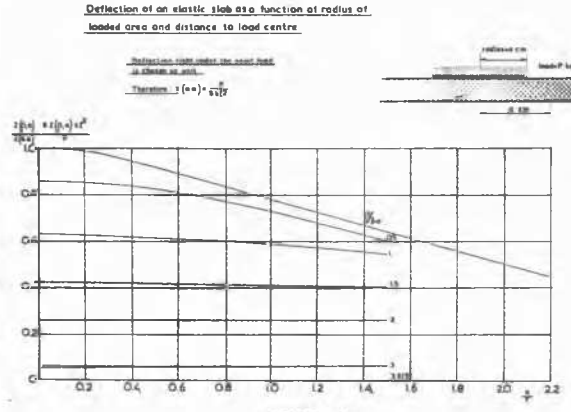

FIG. 6

$$z_{0,0} = \frac{P}{8k\ell^2} \qquad (3,2)$$

Fig. 6 gives the deflection $z_{\rho,a}$ at a distance ρ from the centre for various values of $\frac{a}{\ell}$ and $\frac{\rho}{\ell}$ as a fraction of this z_{00}.

It will be seen that the curves in this figure for higher values of $\frac{\rho}{\ell}$ run practically horizontal, i.e. at some distance from the centre already the deflection differs only little from the deflection in the case of a point load ($\frac{a}{\ell} = 0$) of the same magnitude. With the aid of the graph it is a simple matter to calculate the curve of deflection for any case.

4. CALCULATION OF THE SCHIPHOL "SANDWICH" CONSTRUCTION.

The further calculation of the Schiphol construction with the aid of the preceding is now obvious. We go back to fig. 1, where the pressure distribution in the cement concrete slab is given both for the single and for the dual wheel.

This bell-shaped curve (we take a separate wheel of the dual system and not the two wheels together) is now approximated with a set of cylindrical disks of a slight thickness Each disk represents a homogeneous load of 0.4

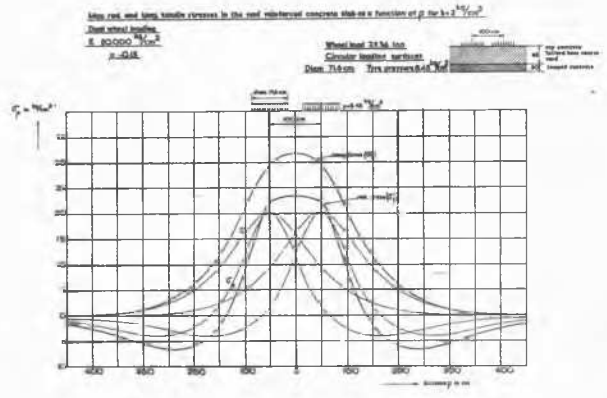

FIG. 7

kg/cm^2 distributed over a circular area with a continually decreasing radius.

For each of these disks the total load it represents was determined and then the corresponding tangential and radial tensile stresses in each point of the slab could be calculated. By adding up the values of all disks we find the total tangential and radial tensile stress curves.

In fig. 7 the result of this procedure is given for the case of a dual wheel with a wheel distance of 100 cm. The curve is easily found by calculating the tensil stress curve for one of the two wheels, shifting it 100 cm and adding the two. The maximum tensile stress actually occurs between the two wheels. It may be seen from fig. 7 that the σ_t curve is less steep than that for σ_ρ. Consequently, the maximum for the total σ_t curve is higher than that for the σ_ρ curve. This means that the maximum of this total σ_t curve represents at the same time the maximum tensile stress occurring in the slab for the case of dual-wheel loading. This may be clear from the following. In the preceding section it was already pointed out that at the upper and lower surfaces of the

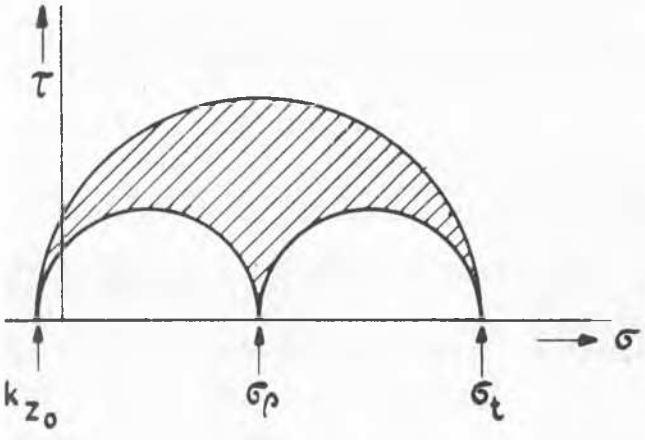

FIG. 8

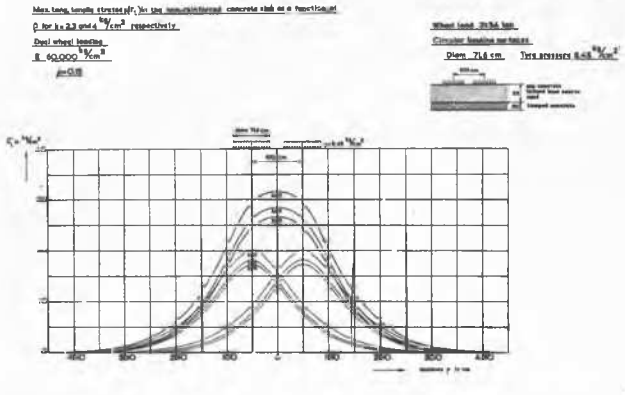

FIG. 9

slab for which our calculations were made σ_t and σ_p are principal stresses. For the upper side of the slab the third principal stress is the stress in the zero point of fig. 1, so about 2.7 kg/cm2, and for the lower side it is the counterpressure of the soil, which, as will be seen below, is less than 1 kg/cm2, These figures are low with respect to those for σ_p and σ_t. Mohr's stress diagram now shows the following picture (fig. 8).

The shaded area comprises the appurtenant values of shearing and tensile stresses. It will be easily seen that the greatest principal stress σ_t must also be the maximum tensile stress.

In fig. 9 curves are given for values of k = 2, 3 and 4 kg/cm3 respectively.

The same procedure may be followed for the case of single-wheel loading, but here only the stresses under the load centre need be calculated

Calculations are carried out for a value of E = 60,000 kg/cm2.

The results for single- and dual-wheel loading may be compared from fig. 10.

It may be seen from this figure that dual-wheel loading gives a considerable decrease in stresses.

For a wheel distance of 160 cm, which is an acceptable value, we find that the stresses are reduced by a factor 0.7 as compared with singlewheel loading.

In the calculations given there remain two elements of some uncertainty.

First, it is doubtful whether the cement-

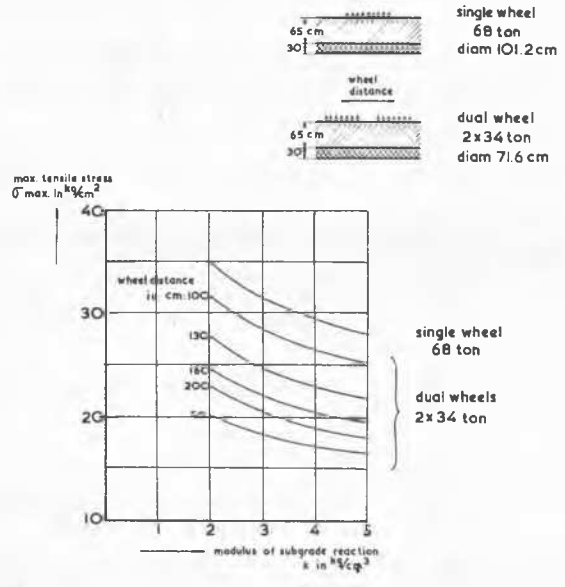

FIG. 10

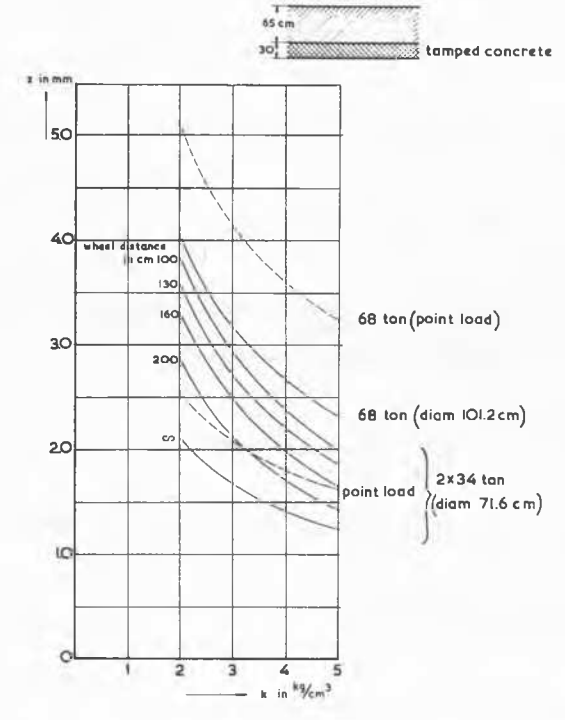

FIG. 11

concrete slab may be regarded as a perfect rigid boundary. Secondly, the description of the influence of the subsoil with a constant modulus of subgrade reaction may give too rough a picture of the actual behaviour.

Here the final word rests with the experiment. It is clear, however, that the method of calculation remains quite the same, when another pressure-distribution on the cement-concrete slab occurs.

At any rate the stresses calculated here are on the safe side and give a good comparison between the cases of dual and single wheel loading.

5. DEFLECTIONS

The maximum deflections of the concrete slab are calculated in the same way as described above. The results are given in fig.11.

6. CALCULATION OF THE MAXIMUM STRESSES AND DEFLECTIONS IN AN INFINITE SLAB ON AN ELASTIC BASE UNDER AN ARBITRARY LOAD.

6,1 Derivation of the general form of the solution.

The equation for the deflection z of the neutral plane is:

$$\frac{m^2E}{m^2-1}\cdot\frac{h^3}{12}\cdot\Delta\Delta z = -kz + p \qquad (6.1.1)$$

where: E = modulus of elasticity (Young's modulus)
m = Poisson's constant
h = thickness of the slab
z = deflection
p = local pressure on top of the slab
k = modulus of subgrade reaction.

In the case of radial symmetry it obtains for the maximum bending stress in radial direction that:

$$\sigma_r = -\frac{m^2E}{m^2-1}\cdot\frac{h}{2}\cdot\left(\frac{\delta^2 z}{\delta r^2}+\frac{1}{m}\cdot\frac{1}{r}\cdot\frac{\delta z}{\delta r}\right) =$$

$$= -\frac{m^2E}{m^2-1}\cdot\frac{h}{2}\left(\Delta z + \frac{1-m}{m}\cdot\frac{1}{r}\frac{\delta z}{\delta r}\right) \qquad (6.1.2)$$

In the case of radial symmetry the boundary conditions are valid:

$$r = 0, \frac{\delta z}{\delta r} = 0 \text{ and } \frac{\delta \Delta z}{\delta r} = 0 \quad \text{z finite and bending stress maximum}$$

$$r = \infty,\ z = \frac{\delta z}{\delta r} = 0,\ \Delta z = 0 \qquad (6.1.3)$$

In the infinite, deflection and shearing stresses must be zero.

Equation (6.1.1) is written:

$$\Delta\Delta z = -\lambda^4 z + q \qquad (6.1.4)$$

where, $\lambda^4 = \frac{m^2-1}{m^2E}\cdot\frac{12}{h^3}\cdot k$ and

$$q = \frac{m^2-1}{m^2E}\cdot\frac{12}{h^3}\cdot p = \lambda^4\cdot\frac{p}{k} \qquad (6.1.5)$$

To solve equation (6.1.4) we put:

$$\Delta z - i\lambda^2 z = u \quad \text{or} \quad \Delta z = u + i\lambda^2 z \qquad (6.1.6)$$

Then (6.1.4) passes into:

$$\Delta\Delta z = u + i\lambda^2\Delta z = \Delta u + i\lambda^2 u - \lambda^4 z = -\lambda^4 z + q$$

$$\text{or} \quad \Delta u + i\lambda^2 u = q \qquad (6.1.7)$$

After solving u from this substitution into (6.1.6) produces the equation of (z). Equations (6.1.6) and (6.1.7) are of the same type.

In the case of radial symmetry equation (6.1.7) is;

$$\frac{1}{r}\frac{d}{dr}\left(r\frac{du}{dr}\right) + i\lambda^2 u = q(r) \qquad (6.1.8)$$

with the boundary conditions:

$$r = 0 \qquad u \text{ finite and } r\frac{du}{dr} = 0 \qquad (6.1.9)$$

$$r = \infty \qquad u = 0$$

We solve this equation with the aid of a Green function $G(r,\xi)$. This function satisfies the homogeneous differential equation:

$$\frac{1}{r}\frac{d}{dr}\left(r\frac{dG}{dr}\right) + i\lambda^2 G = 0 \qquad (6.1.10)$$

the boundary conditions (6.1.9) and, moreover, the requirement that at the point ξ it obtains that:

$$r\frac{dG}{dr}\Big/_{\xi+0} - r\frac{dG}{dr}\Big/_{\xi-0} = -1 \qquad (6.1.11)$$

By partial integration we find:

$$u(\xi) = \int_0^\infty G(\xi,r).\,q(r).r.dr. \qquad (6.1.12)$$

When $u(\xi)$ is found, z is obtained from (6.1.6) in the same way with the aid of a Green function $H(\rho,\xi)$ for the differential equation

$$\frac{1}{\xi}\cdot\frac{d}{d\xi}\left(\xi\frac{dH}{d\xi}\right) - i\lambda^2 H = 0 \qquad (6.1.13)$$

with the boundary conditions;

$$\xi = 0 \qquad H \text{ finite } \frac{dH}{d\xi} = 0$$

$$\xi = \infty \qquad H = 0$$

and the requirement that for $\xi = \rho$ it obtains that:

$$\xi\frac{dH}{d\xi}\Big/_{\rho+0} - \xi\frac{dH}{d\xi}\Big/_{\rho-0} = -1 \qquad (6.1.14)$$

By analogy to (6.1.12) we find:

$$z(\rho) = \int_0^\infty H(\rho,\xi).\,u(\xi).\,\xi.\,d\xi \qquad (6.1.15)$$

or:

$$z(\rho) = \int_0^\infty\int_0^\infty H(\rho,\xi).\,G(\xi,r).\,q(r)\,r\,dr.\,\xi\,d\xi \qquad (6.1.16)$$

This double integral can be written as:

$$z(\rho) = \int_0^\infty K(\rho,r).\,q(r).\,r\,dr \qquad (6.1.17)$$

where,

$$K(\rho,r) = \int_0^\infty H(\rho,\xi).\,G(\xi,r).\,\xi\,d\xi \qquad (6.1.18)$$

6.2 Calculation of the Green functions.

The solution of equation (6.1.10) which satisfies the boundary conditions for r = 0 is $Jo(\lambda r\sqrt{i})$, the solution which satisfies the boundary conditions for $r = \infty$ is $Ho^{(1)}(\lambda r\sqrt{i})$.

Substituting these functions and taking into account the condition (6.1.11) we find:

$$G(r,\xi) = \begin{cases} \frac{\pi}{2}\,i.\,Jo(\lambda r\sqrt{i}).Ho^{(1)}(\lambda\xi\sqrt{i}) & r < \xi \\ \frac{\pi}{2}\,i.\,Ho^{(1)}(\lambda r\sqrt{i}).Jo(\lambda\xi\sqrt{i}) & r > \xi \end{cases} \qquad (6.2.1)$$

In an analogous way we find for the function $H(\rho,r)$ (by replacing i by -i):

$$H(\rho,r) = \begin{cases} -\frac{\pi}{2}\,i.Jo(\lambda r\sqrt{-i}).Ho^{(1)}(\lambda\rho\sqrt{-i}) & r < \rho \\ -\frac{\pi}{2}\,i.Ho^{(1)}(\lambda r\sqrt{-i}).Jo(\lambda\rho\sqrt{-i}) & r > \rho \end{cases} \qquad (6.2.2)$$

The function $K(\rho.r)$ given by (6.1.18) can be reduced with the aid of equation (6.1.10) which is satisfied by $G(\xi.r)$ and taking into account that $G(\xi,r)$ is symmetrical in ξ and r.
For, partial integration results in:

$$K(\rho,r) = \int_0^\infty H(\rho,\xi).G(\xi,r).\xi d\xi = \frac{-i}{2\lambda^2}\{H(\rho,r)-G(\rho,r)\} \tag{6.2.3}$$

$$\text{or : } K(\rho,r) = \frac{\pi}{2\lambda^2}\begin{Bmatrix}\mathrm{Re}\{Jo(\lambda r\sqrt{i})\ Ho^{(1)}(\lambda\rho\sqrt{i})\}\\ \mathrm{Re}\{Jo(\lambda\rho\sqrt{i})\ Ho^{(1)}(\lambda r\sqrt{i})\}\end{Bmatrix} =$$

$$= \frac{\pi}{2\lambda^2}\begin{cases}\mathrm{Re}\ Jo(\lambda r\sqrt{i}).\mathrm{Re}\ Ho^{(1)}(\lambda\rho\sqrt{i}) + \\ \mathrm{Re}\ Jo(\lambda\rho\sqrt{i}).\mathrm{Re}\ Ho^{(1)}(\lambda\rho\sqrt{i}) - \\ \quad + \mathrm{Im}\ Jo(\lambda r\sqrt{i}).\mathrm{Im}\ Ho^{(1)}(\lambda\rho\sqrt{i}) \quad r<\rho \\ \quad - \mathrm{Im}\ Jo(\lambda\rho\sqrt{i}).\mathrm{Im}\ Ho^{(1)}(\lambda r\sqrt{i}) \quad r>\rho\end{cases} \tag{6.2.4}$$

The functions occurring Here have been tabulated by Jahnke and Emde, p.296 and ff. 6)

6.3 Calculation of the stresses and deflections

With the aid of the formula (6.2.4) for $K(\rho,r)$ and (6.1.17) $z(\rho)$ can be calculated for any point of the slab.

The stresses are more important. The tangential and radial stresses are given by

$$\sigma_t = -\frac{m^2E}{m^2-1}.\frac{h}{2}\left\{\frac{1}{m}.\frac{\delta^2 z}{\delta\rho^2}+\frac{1}{\rho}.\frac{\delta z}{\delta\rho}\right\} \tag{6.3.1}$$

and the formulae (6.1.2), which we now write in the following form:

$$\frac{m^2-1}{m^2E}.\frac{2}{h}.\sigma_t = -\left\{\frac{\Delta z}{m}-\frac{1-m}{m}.\frac{1}{\rho}.\frac{\delta z}{\delta\rho}\right\} \tag{6.3.2}$$

$$\frac{m^2-1}{m^2E}.\frac{2}{h}.\sigma_\rho = -\left\{\Delta_\rho z+\frac{1-m}{m}.\frac{1}{\rho}.\frac{\delta z}{\delta\rho}\right\} \tag{6.3.3}$$

We will make the further calculations for the radial stress σ_ρ; the calculation of σ_t is analogous.

With the aid of the formula (6.1.17) for z, (6.2.3) for K (6.1.10) and (6.1.13), formula (6.3.3) is reduced to:

$$\frac{m^2-1}{m^2E}.\frac{2}{h}.\sigma_\rho =$$

$$= -\tfrac{1}{2}\int_0^\infty\{H(\rho,r)+G(\rho,r)\}.q(r).r.dr +$$

$$\frac{i(1-m)}{2\lambda^2 m}.\frac{1}{\rho}\int_0^\infty\frac{\delta}{\delta\rho}\{H(\rho,r)-G(\rho,r)\}\ q(r).r.dr \tag{6.3.4}$$

In particular, we consider the case that the case $q(r)$ is constant over a circular area with radius R and is zero outside it.

$q(r) = q \quad 0<r<R.$

$q(r) = 0 \quad r>R.$

In this case the deflection is:

$$z(\rho,R) = q\int_0^R K(\rho,r)r.dr =$$

$$= \frac{-qi}{2\lambda^2}\int_0^R\{H(\rho,r)-G(\rho,r)\}r.dr \tag{6.3.5}$$

With the aid of (6.1.13) and (6.1.10) this is reduced to:

$$z(\rho,R) = -\frac{qi}{2\lambda^2}\left\{\frac{1}{i\lambda^2}\int_0^R d\left[r.\frac{dH(\rho,r)}{dr}\right]+\right.$$

$$\left.+\frac{1}{i\lambda^2}\int_0^R d\left[r\frac{dG(\rho,r)}{dr}\right]\right\} =$$

$$= \frac{q}{2^4}\left\{\int_0^R d\left[r\frac{dH(\rho,r)}{dr}\right]+\int_0^R d\left[r\frac{dG(\rho,r)}{dr}\right]\right\} \tag{6.3.6}$$

From this it follows by means of partial integration:

$$z(\rho,R) = \frac{qR}{2^4}\begin{cases}\dfrac{dH(\rho,R)}{dR}+\dfrac{dG(\rho,R)}{dR}+\dfrac{2}{R} & R>\rho\\ \dfrac{dH(\rho,R)}{dR}+\dfrac{dG(\rho,R)}{dR} & R<\rho\end{cases} \tag{6.3.7}$$

Substitution of (6.2.1) and (6.2.2) results in

$$z(\rho,R) = \frac{\pi qRi}{2\lambda^3}\begin{cases}-i\mathrm{Im}\sqrt{i}.H_1^{(1)}(\lambda R\sqrt{i}).Jo(\lambda\rho\sqrt{i})+\\ \qquad +\dfrac{2}{\pi iR\lambda} & R>\rho\\ -i\mathrm{Im}\sqrt{i}.H_0^{(1)}(\lambda\rho\sqrt{i}).J_1(\lambda R\sqrt{i}) & R<\rho\end{cases} \tag{6.3.8}$$

Particularly from this it follows for $\rho = 0$ that

$$z(o,R) = \frac{\pi qR}{2\lambda^3}\left\{\frac{2}{\pi R}+\mathrm{Im}\sqrt{i}.H_1^{(1)}(\lambda R\sqrt{i})\right\} \tag{6.3.9}$$

The stresses are found from the formula (6.3.4), which for this load assume the form:

$$\frac{m^2-1}{m^2E}.\frac{2}{h}.\sigma_\rho = -\tfrac{1}{2}q\int_0^R\{H(\rho,r)+G(\rho,r)\}.r.dr+$$

$$+\frac{i(1-m)}{2\lambda^2 m}.\frac{q}{\rho}.\frac{\delta}{\delta\rho}\int_0^R\{H(\rho,r)-G(\rho,r)\}.r.dr =$$

$$= -\tfrac{1}{2}q\left\{\frac{1}{i\lambda^2}\int_0^R d\ r\frac{dH(\rho,r)}{dr}-\frac{1}{i\lambda^2}\int_0^R d\ r\frac{dG(\rho,r)}{dr}\right\}+$$

$$+\frac{i(1-m)}{2\lambda^2 m}.\frac{q}{\rho}.\frac{\delta}{\delta\rho}\left\{\frac{1}{i\lambda^2}\int_0^R d\ r\frac{dH(\rho,r)}{dr}+\right.$$

$$+\frac{1}{i\lambda^2}\int_0^R d\,r\frac{dG(\rho,r)}{dr}\Bigg\} =$$

$$= -\frac{qR}{2i\lambda^2}\left\{\frac{\delta H(\rho,R)}{\delta R} - \frac{\delta G(\rho,R)}{\delta R}\right\} +$$

$$+\frac{(1-m)qR}{2\lambda^4 m}\cdot\frac{1}{\rho}\cdot\left\{\frac{\delta^2 H(\rho,R)}{\delta\rho\,\delta R} + \frac{\delta^2 G(\rho,R)}{\delta\rho\,\delta R}\right\} \qquad (6.3.10)$$

Substitution of the expressions for G and H gives:

$$\frac{m^2-1}{m^2E}\cdot\frac{2}{h}\cdot\sigma_\rho =$$

$$= -\frac{\pi}{2}\cdot\frac{qR}{\lambda}\left\{\begin{matrix}\mathrm{Re}\left\{\sqrt{i}\;J_1(\lambda R\sqrt{i})\,.\,H_0^{(1)}(\lambda\rho\sqrt{i})\right\}\\ \\ \mathrm{Re}\left\{\,i\;H_1^{(1)}(\,R\,i)\,.J_0(\lambda\rho\sqrt{i})\right\}\end{matrix}\right. -$$

$$-\frac{(1-m)qR}{2\lambda^2 m\,\rho}\left\{\begin{matrix}\mathrm{Re}\left\{J_1(\lambda R\sqrt{i})\,.\,H_1^{(1)}(\lambda\rho\sqrt{i})\right\} & R<\rho\\ \\ \mathrm{Re}\left\{J_1(\lambda\rho\sqrt{i})\,.\,H_1^{(1)}(\lambda R\sqrt{i})\right\} & R>\rho\end{matrix}\right. \qquad (6.3.11)$$

For a further elaboration we write this as follows:

$$\frac{m^2-1}{m^2E}\cdot\frac{2}{h}\cdot\sigma_\rho = -\frac{\pi}{2}\frac{qR}{\lambda}|\alpha| - \frac{\pi(1-m)qR}{2\lambda^2 m\rho}|\beta| \qquad (6.3.12)$$

To compare these results with the formulae found by H.M. Westergaard (Stresses in concrete runways of airports 2)), we substitute other symbols, viz.:

acc. to Westergaard	Here:
ℓ	$\frac{1}{\lambda}$
P	$p.\pi R^2 = \frac{k\,\pi\,qR^2}{\lambda^4}$ (see 6.1.5)
a	R
μ	$\frac{1}{m}$

In this way we find:

$$\frac{\sigma_\rho h^2}{P} = 3\frac{\ell}{a}\left[(1-\mu)\frac{\ell}{a}|\beta| - |\alpha|\right] \qquad (6.3.13)$$

Similarly we find for the tangential stress:

$$\frac{\sigma_t h^2}{P} = 3\frac{\ell}{a}\left[-(1-\mu)\frac{\ell}{\rho}|\beta| - \frac{|\alpha|}{m}\right] \qquad (6.3.14)$$

The meaning of $|\beta|$ and $|\alpha|$ follows from (6.3.11) and (6.3.12). To reach functions which have been tabulated by Jahnke and Emde it is necessary to rewrite these formulae.
After simple elaborations we find:

$$|\beta| = \left\{\mathrm{Im}\sqrt{i}\;J_1\left(\frac{a}{\ell}i\right)\right\}\left\{\mathrm{Re}\sqrt{i}\;H_1^{(1)}\left(\frac{\rho}{\ell}\sqrt{i}\right)\right\} +$$

$$\left\{\mathrm{Im}\sqrt{i}\;J_1\left(\frac{\rho}{\ell}\sqrt{i}\right)\right\}\left\{\mathrm{Re}\sqrt{i}\;H_1^{(1)}\left(\frac{a}{\ell}\sqrt{i}\right)\right\} +$$

$$+\left\{\mathrm{Re}\sqrt{i}\;J_1\left(\frac{a}{\ell}\sqrt{i}\right)\right\}\left\{\mathrm{Im}\sqrt{i}\;H_1^{(1)}\left(\frac{\rho}{\ell}\sqrt{i}\right)\right\} \quad \frac{a}{\ell}<\frac{\rho}{\ell}$$

$$+\left\{\mathrm{Re}\sqrt{i}\;J_1\left(\frac{\rho}{\ell}\sqrt{i}\right)\right\}\left\{\mathrm{Im}\sqrt{i}\;H_1^{(1)}\left(\frac{a}{\ell}\sqrt{i}\right)\right\} \quad \frac{a}{\ell}>\frac{\rho}{\ell} \qquad (6.3.15)$$

$$|\alpha| = \left\{\mathrm{Re}\sqrt{i}\;J_1\left(\frac{a}{\ell}\sqrt{i}\right)\right\}\left\{\mathrm{Re}\;H_0^{(1)}\left(\frac{\rho}{\ell}\sqrt{i}\right)\right\} -$$

$$\left\{\mathrm{Re}\sqrt{i}\;H_1^{(1)}\left(\frac{a}{\ell}\sqrt{i}\right)\right\}\left\{\mathrm{Re}\;J_0\left(\frac{\rho}{\ell}\sqrt{i}\right)\right\} -$$

$$-\left\{\mathrm{Im}\sqrt{i}\;J_1\left(\frac{a}{\ell}\sqrt{i}\right)\right\}\left\{\mathrm{Im}\;H_0^{(1)}\left(\frac{\rho}{\ell}\sqrt{i}\right)\right\} \quad \frac{a}{\ell}<\frac{\rho}{\ell}$$

$$-\left\{\mathrm{Im}\sqrt{i}\;H_1^{(1)}\left(\frac{a}{\ell}\sqrt{i}\right)\right\}\left\{\mathrm{Im}\;J_0\left(\frac{\rho}{\ell}\sqrt{i}\right)\right\} \quad \frac{a}{\ell}>\frac{\rho}{\ell} \qquad (6.3.16)$$

With (6.3.15) and (6.3.16) the radial and tangential stresses can be calculated directly with the aid of the collection of tables mentioned.

In the special case for $\rho = 0$ the tangential and radial stresses are equal ($\sigma_\rho = \sigma_t = \sigma_o$) and have their maximum value. From (6.3.11) it follows using the other symbols:

$$\frac{\sigma_o h^2}{P} = -\frac{3(1+\mu)}{2}\cdot\frac{\ell}{a}\cdot\mathrm{Re}\left\{\sqrt{i}\;H_1^{(1)}\left(\frac{a}{\ell}\sqrt{i}\right)\right\} \qquad (6.3.17)$$

This may be rewritten as:

$$\sigma_o = -\frac{3(1+\mu)}{2}\cdot\frac{P}{h^2\sqrt{2}}\cdot\frac{\ell}{a}\,(\mathrm{Re}-\mathrm{Im})\left\{H_1^{(1)}\frac{a}{\ell}\sqrt{i}\right\} \qquad (6.3.18)$$

which formula is identical with Westergaard's 2). It is more accurate, however, to use formula (6.3.17) as the functions of (6.3.18)are only given graphically by Jahnke and Emde and, in addition, subtraction may give rise to considerable errors.

From the formulae it will be seen immediately that the results of these calculations give the dimensionless stress magnitudes

$\frac{\sigma_\rho h^2}{P}$ and $\frac{\sigma_t h^2}{P}$ as functions of $\frac{a}{\ell}$ and $\frac{\rho}{\ell}$

which are also dimensionless magnitudes.

From figures 3, 4 and 5, which have been computed with the aid of the formulae (6.3.13), (6.3.14) and (6.3.17), the dimensionless stress magnitudes can be directly derived. It is then very easy to calculate the stresses from these.

If we write formula (6.3.8) with the Westergaard symbols we find after some elaboration to reach tabulated functions:

$$\frac{8z(\rho,a)k^2}{P} =$$

$$4\frac{\ell}{a}\cdot\left[\begin{array}{l}\left\{\mathrm{Im}\sqrt{i}\,H_1^{(1)}\left(\frac{a}{\ell}\sqrt{i}\right)\right\}\left\{\mathrm{Re}\,J_0\left(\frac{\rho}{\ell}\sqrt{i}\right)\right\}+\\ \left\{\mathrm{Im}\,H_0^{(1)}\left(\frac{\rho}{\ell}\sqrt{i}\right)\right\}\left\{\mathrm{Re}\sqrt{i}\,J_1\left(\frac{a}{\ell}\sqrt{i}\right)\right\}+\\ +\left\{\mathrm{Re}\sqrt{i}\,H_1^{(1)}\left(\frac{a}{\ell}\sqrt{i}\right)\right\}\left\{\mathrm{Im}\,J_0\left(\frac{\rho}{\ell}\sqrt{i}\right)\right\}+\frac{2\ell}{\pi a} \quad \frac{a}{\ell}>\frac{\rho}{\ell}\\ +\left\{\mathrm{Re}\,H_0^{(1)}\left(\frac{\rho}{\ell}\sqrt{i}\right)\right\}\left\{\mathrm{Im}\sqrt{i}\,J_1\left(\frac{a}{\ell}\sqrt{i}\right)\right\} \quad \frac{a}{\ell}<\frac{\rho}{\ell}\end{array}\right. \qquad (6.3.19)$$

For the deflection under the centre of loading (6.3.9) is valid. After rewriting this in the other way we find for the deflection under the load centre:

$$\frac{8z(0,a)k\ell^2}{P}=\frac{8}{\pi}\left(\frac{\ell\rho}{a}\right)+4\frac{\ell}{a}\left\{\mathrm{Im}\sqrt{i}\,H_1^{(1)}\left(\frac{a}{\ell}\sqrt{i}\right)\right\} \qquad (6.3.20)$$

In the case of a point load ($\frac{a}{\ell}=0$) both (6.3.19) and (6.3.20) lose their validity. For $R<\rho$ (6.3.8) may be written as:

$$z(\rho,a)=\frac{Pi}{2a\ell k}\left\{-i\,\mathrm{Im}\sqrt{i}\,H_0^{(1)}\left(\frac{\rho}{\ell}\sqrt{i}\right)J_1\left(\frac{a}{\ell}\sqrt{i}\right)\right\} \qquad (6.3.21)$$

For low values of a it obtains that:

$$J_1\left(\frac{a}{\ell}\sqrt{i}\right)=\tfrac{i}{2}\frac{a}{\ell}\sqrt{i}$$

therefore:

$$z(\rho,0)=\frac{P}{4k\ell^2}\left[\mathrm{Im}\left\{i\,H_0^{(1)}\left(\frac{\rho}{\ell}\sqrt{i}\right)\right\}\right]$$

or

$$\frac{8z(\rho,0)k\ell^2}{P}=2\,\mathrm{Re}\left\{H_0^{(1)}\left(\frac{\rho}{\ell}\sqrt{i}\right)\right\} \qquad (6.3.22)$$

For the deflection under the centre of the point load z_{00} we find from (6.3.22): ($a=\rho=0$)

$$\frac{8z(0,0)k\ell^2}{P}=1 \qquad (6.3.23)$$

Just as in the case of the stress formulae here, too, the deflections can be expressed in dimensionless magnitudes. The dimensionless magnitude of the deflection is here $8zk^2/P$, which can be calculated as a function of a/ℓ and ρ/ℓ from formulae (6.3.19), (6.3.20), and (6.3.22). The dimensionless magnitude of the deflection has been chosen in such a way that it becomes equal to unity for the deflection under the centre of a point load.

With the aid of the above-mentioned formulae figure 6 has been made, from which the desired deflections can be easily calculated. If we convert our formula (6.3.20) for the deflection under the centre of the loaded area in the same way as was done with (6.3.17), we obtain:

$$z(0,a)=\frac{P}{2k\ell^2}\left\{\frac{\ell}{a\sqrt{2}}(\mathrm{Re}+\mathrm{Im})\,H_1^{(1)}\left(\frac{a}{\ell}\sqrt{i}\right)+\frac{2}{\pi}\left(\frac{\ell}{a}\right)^2\right\} \qquad (6.3.24)$$

which is identical with the formulae given by Westergaard 2).

Here again, however, it is easier and more accuate to use (6.3.20).

LIST OF LITERATURE

1) H. Hertz, Ueber das Gleichgewicht schwimmender elastischer Platten. Ann. d. Phys. 22,449, 1884. Gesammelte Werke s. 288.
2) H.M. Westergaard, Proc. Highway Res. Board 19, 197, 1939.
3) Cummings, Foundation stresses in an Elastic Solid with a Rigid Underlying Boundary, Civil Eng. vol. 11, p.666-667 (1941)
4) Karl Terzaghi, Theoretical Soil Mechanics. London, New York 1944, p.420-421.
5) Newmark, Estimating earth pressures. Eng. News Record 120, 23, 1938 .
6) Jahnke und Emde, Tables of functions, from p.296.

-o-o-o-o-o-o-o-